

Interannual Variation of Multiple Tropical Cyclone Events in the Western North Pacific

GAO Jianyun^{*1} (高建芸) and Tim LI² (李天明)

¹*Fujian Climate Center, China Meteorological Administration, Fuzhou 350001*

²*International Pacific Research Center and Department of Meteorology, University of Hawaii, Honolulu, Hawaii*

(Received 14 December 2011; revised 7 June 2012)

ABSTRACT

The interannual variability of occurrence of multiple tropical cyclone (MTC) events during June–October in the western North Pacific (WNP) was examined for the period 1979–2006. The number of the MTC events ranged from 2 to 9 per year, exhibiting a remarkable year-to-year variation. Seven active and seven inactive MTC years were identified. Compared to the inactive years, tropical cyclone genesis locations extended farther to the east and in the meridional direction during the active MTC years. A composite analysis shows that inactive MTC years were often associated with the El Niño decaying phase, as warm SST anomalies in the equatorial eastern-central Pacific in the preceding winter transitioned into cold sea surface temperature (SST) anomalies in the concurrent summer. Associated with the SST evolution were suppressed low-level cyclonic vorticity and weakened convection in the WNP monsoon region.

In addition to the mean flow difference, significant differences between active and inactive MTC years were also found in the strength of the atmospheric intraseasonal oscillation (ISO). Compared with inactive MTC years, ISO activity was much stronger along the equator and in the WNP region during active MTC years. Both westward- and northward-propagating ISO spectrums strengthened during active MTC years compared to inactive years. The combined mean state and ISO activity changes may set up a favorable environment for the generation of MTC events.

Key words: multiple tropical cyclone events, interannual variation

Citation: Gao, J. Y., and T. Li, 2012: Interannual variation of multiple tropical cyclone events in the western North Pacific. *Adv. Atmos. Sci.*, **29**(6), 1279–1291, doi: 10.1007/s00376-012-1031-1.

1. Introduction

With statistical tropical cyclone (TC) distribution map, in 1968 Gray showed that the western North Pacific (WNP) region undergoes the most frequent TC activity among eight TC genesis regions in the world, and the WNP represents 36% of the total TCs globally. Some years later, Gray (1977) investigated the environmental conditions around the cyclogenesis regions and described six physical parameters for evaluating TC genesis potential: (1) a positive relative vorticity in lower troposphere, (2) a location away from the equator, (3) a warm SST >26.1°C, (4) a small vertical shear, (5) a large equivalent potential temperature gradient between 500 hPa and the surface, and (6) a relatively large relative humidity in the middle troposphere. Two decades later, Briegel and Frank (1997)

added that upper-level troughs and low-level southwesterly surges were favorable for TC genesis. Ritchie and Holland (1999) further documented environmental flow regimes that favor TC genesis in the WNP: the monsoon shear line, the monsoon confluence region, and the monsoon gyre.

Whereas the mean flow provides a favorable environment for TC genesis, synoptic-scale precursor perturbations trigger individual TC events. So far, three types of low-level precursor perturbations have been identified in the WNP (Fu et al., 2007): (1) TC energy dispersion induced Rossby wave train (Ritchie and Holland, 1999; Sobel and Bretherton, 1999; Li et al., 2003; Li and Fu, 2006), (2) easterly waves (Chang et al., 1970; Tam and Li, 2006; Fu et al., 2007), and (3) northwest–southeast-oriented tropical-depression (TD)-type disturbances that are not caused

^{*}Corresponding author: GAO Jianyun, fzgaojyun@163.com

by the energy dispersion of preexisting TCs (Lau and Lau, 1990; Takayabu and Nitta, 1993; Chang et al., 1996; Dickinson and Molinari, 2002; Li, 2006). TC genesis in the WNP is largely modulated by large-scale, low-frequency systems such as the Madden-Julian Oscillation (MJO) (Nakazawa, 1988; Liebmann et al., 1994; Harr and Elsberry, 1995a, b; Sobel and Maloney, 2000; Chen et al., 2000; Maloney and Dickinson, 2003; Camargo et al., 2007a, b; Kim et al., 2008) and the El Niño-Southern Oscillation (ENSO) (Chan, 1985; Lander, 1994; Chen et al., 1998; Saunders et al., 2000; Wang and Chan, 2002; Chia and Ropelewski, 2002; Wu et al., 2004; Camargo and Sobel, 2005; Camargo et al., 2007a, c). In addition, TC activity in the WNP may be also affected by remote signals such as Antarctic Oscillation (AAO), Asia-Pacific Oscillation (APO), North Pacific Oscillation (NPO), North Pacific sea ice cover, Hadley Circulation, and SST anomalies east of Australia (Wang and Fan, 2007a, b; Fan, 2007; Zhou et al., 2008; Zhou and Cui, 2008, 2011).

In the Indian Ocean and the western Pacific, pre-dominant 10–20-day periodicity has been detected in precipitation and wind fields from spectral analyses (Murakami and Frydrych, 1974; Zangvil, 1975; Murakami, 1976; Krishnamurti and Bhalme, 1976; Krishnamurti and Ardanuy, 1980; Chen and Chen, 1993; Kiladis and Wheeler, 1995; Numaguti, 1995) and this quasi-biweekly variation is sometimes viewed as a high-frequency part of the tropical intraseasonal oscillation (ISO; Zhang, 2005; Waliser, 2006). Nakazawa (1986) reported that TC formation tends to occur more frequently during the active phase of ISO at both the 15–25-day and 30–60-day time scales in both Northern and Southern Hemisphere summers. The MJO–ENSO relationship has also been investigated extensively in several studies (e.g., Lau and Shen, 1988; Teng and Wang, 2003; Hendon et al., 2007; Lin and Li, 2008; Shi et al., 2009). Frank and Roundy (2006) analyzed relationships between tropical wave activity and tropical cyclogenesis in the Earth's major TC basins. In addition to their large-scale impact, TCs do not form evenly across time; they have a tendency to cluster in some periods (Krouse and Sobel, 2009; Gao and Li, 2010). Krouse and Sobel (2010) examined TC clustering processes related to successive TC energy dispersion. Gao and Li (2010) defined a more general term of a multiple tropical cyclone (MTC) event in which two or more TCs form within a relatively short period compared to their statistical value. They found the occurrence of MTC events in the WNP to be largely regulated by the combined large-scale impact of the atmospheric biweekly oscillation (BWO), ISO, and lower-frequency oscillations of 90 days or longer, including ENSO and other interan-

nual modes.

The objective of this study was to document the interannual variation of the occurrence of the MTC events in the WNP. By analyzing the differences in composite circulation and SST patterns between active and inactive MTC years, we have elucidated physical mechanisms that give rise to this interannual variability. The rest of the paper is organized as follows. Section 2 describes the data and methodology. Section 3 shows the observed features of interannual variations of the MTC events. Our analysis of the mechanism responsible for interannual variability is presented in section 4. The relationship between MTC and ENSO is further discussed in section 5. Finally, a conclusion is presented in section 6.

2. Data and methodology

The primary datasets used in this study were acquired from the National Ocean and Atmospheric Administration (NOAA) outgoing longwave radiation data (OLR; Liebmann and Smith, 1996) and the National Centers for Environmental Prediction–Department of Energy (NCEP–DOE) Atmospheric Model Intercomparison Project (AMIP-II) Reanalysis data (Kanamitsu et al., 2002). Both the datasets are global, daily averaged products with $2.5^\circ \times 2.5^\circ$ grid resolution. The monthly mean SST field of the NOAA Extended Reconstructed SST (V3) dataset has a $2^\circ \times 2^\circ$ global grid. The best-track TC data from the Joint Typhoon Warning Center (JTWC) were used to determine TC genesis time and location in the WNP. The typical warning by the Joint Typhoon Warning Center (JTWC) begins when a TC first reaches tropical depression intensity. Because the typhoon peak season in the WNP is from June to October, in this study, we referred to this period as general summer. The MTC analysis in this study was confined to this general summer period from 1979 to 2006, as satellite products have been routinely incorporated into the NCEP assimilation system since 1979 (Kalnay et al., 1996).

A composite analysis method was utilized to reveal the difference of large-scale circulation fields between the active and inactive MTC years. A two-sample Student's *t*-test was adopted to determine the significance of the composite differences of the fields.

To examine the role of the interannual variation of ISO, we applied a Lanczos filter (Duchon, 1979) to the daily OLR and reanalysis fields to extract the intraseasonal (25–70-day) component. A wavenumber-frequency analysis was conducted to transform the OLR field from a space-time domain to a wavenumber-frequency domain. Following Teng and Wang (2003)

and Lin and Li (2008), we applied the wavenumber-frequency analysis to a finite domain (10°S – 30°N , 40° – 180°E), as the boreal summer intraseasonal oscillation (BSISO) convection is effectively trapped in the summer monsoon region by the lower boundary conditions (such as SST and land and ocean surface moisture distribution; Li and Wang, 1994) and the three-dimensional background monsoon flows (Wang and Xie, 1997). Hayashi's (1982) formalism was adopted in the present work; that is, the variances of the intraseasonal anomalies propagating in opposite directions were estimated by the co-spectrum between two Fourier spatial decomposition coefficients. To minimize the effect of discontinuity in the OLR time series, our strategy was to calculate the spectrum for each summer first and then compile a composite for active and inactive MTC years. For the limited domain analysis, zonal wavenumber 1 corresponded to a wavelength of 140° in longitude, and meridional wavenumber 1 corresponded to a wavelength of 40° in latitude. The annual mean and the first four harmonics were removed from the original time series each year (to retain the ISO signal) before the wavenumber-frequency analysis was performed.

3. Observed features of interannual variations of MTC events

3.1 Definition of multiple TC events

In this study, we refined the MTC definition of Gao and Li (2010) in the following two aspects. First, we included the month of October, because TCs in the WNP are still quite active in October. Second, we included a distance constraint. It has been argued that physical mechanisms behind MTC events can be attributed to either synoptic self-triggering or a lower-frequency (such as ISO) forcing scenario. The former involves the successive formation of TCs due to TC energy dispersion (Holland, 1995; Li et al., 2003) or energy accumulation of easterly waves in a critical longitude (Kuo et al., 2001; Tam and Li, 2006). The latter involves the large-scale forcing of the westward-propagating ISO in the WNP, which may trigger the successive formation of TCs during its wet phase (Hsu et al., 2011; Hsu and Li, 2011). In both scenarios, the distance between two or more TCs must be confined within a characteristic length scale.

Based on these considerations, an active MTC phase was defined when two successive TCs occurred at a time interval ≤ 3 days while the distance between the two TCs was < 4000 km. If two or more active MTC phases occurred successively, they were regarded as a single active MTC event. Compared with the work of Gao and Li (2010), our definition ruled out

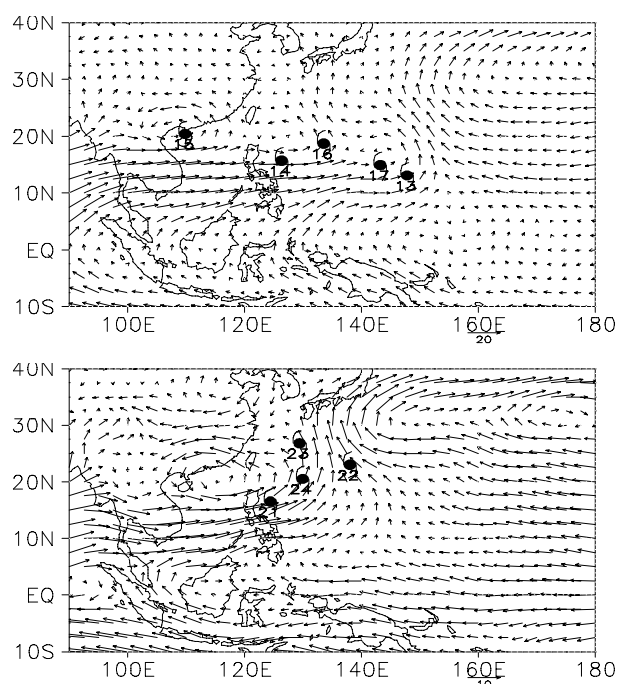


Fig. 1. TC genesis locations (denoted by typhoon signs with named TC numbers written below) and averaged 850-hPa wind (vector) fields during two active MTC periods from 24 July to 1 August 1994 (top) and 10–17 September 1999 (bottom).

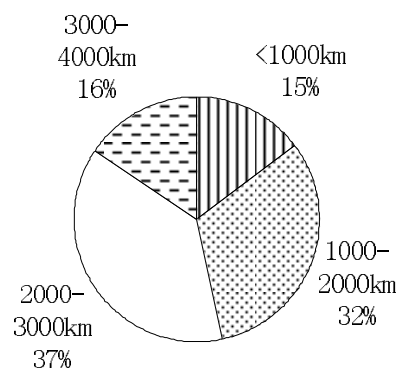


Fig. 2. The percentage of the MTC events as a function of the TC spatial distance.

$\sim 10\%$ of MTC events, which exceeded a distance of 4000 km.

Figure 1 shows two examples of MTC events. In the first example, five TCs formed in a 9-day period; in the second example, four TCs formed in an 8-day period. Notably, the locations of TC genesis appear in either a cyclonic vorticity or a zonal confluence region of low-level background flows averaged during the active MTC periods.

A statistical analysis of the spatial distance be-

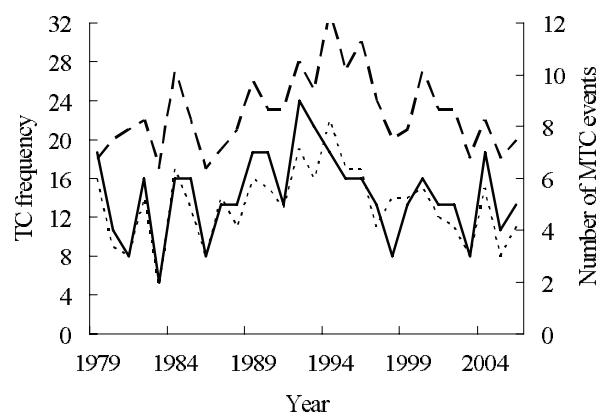


Fig. 3. Time series of the total TC frequency (dashed line) in the WNP, the number of the MTC events (solid line), and the TC number counted during active MTC periods (dotted line) during June–October. The correlation coefficient between the number of MTC events and the TC number occurring during active MTC periods is 0.84, and the correlation coefficient between the number of MTC events and the total TC frequency is 0.65.

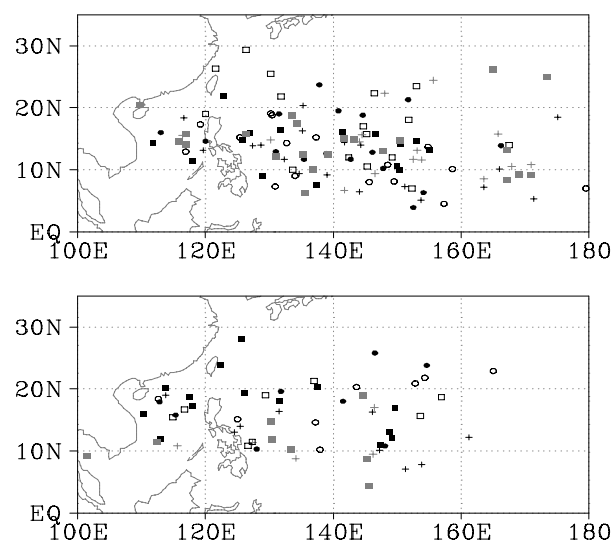


Fig. 4. TC genesis locations associated with all MTC events during the seven active (top panel) and seven inactive (bottom panel) MTC years. Different symbols represent TC locations in different years.

tween the TCs associated with the MTC events (Fig. 2) indicated that $\sim 70\%$ of the MTCs occurred at a distance between 1000 and 3000 km, while $\sim 15\%$ occurred at a distance either <1000 km or >3000 km.

3.2 Active and inactive MTC years

Figure 3 illustrates the time series of the number of MTC events each year, along with the number of TCs counted during the active MTC period and total

TC number in June–October for the period 1979–2006. The number of MTC events shows a marked interannual variation, with nine MTC events appearing in 1992 and only two MTC events in 1983.

The correlation coefficient between the total number of MTC events and TC number during the active MTC period was 0.84, which exceeds a 95% confidence level. The correlation coefficient between the number of MTC events and the total summer TC frequency is 0.65, which also exceeds the 95% confidence level. This implies that more frequent TCs form in summer when the environment favors MTC formation.

For the period 1979–2006, the average number of active MTC events per year was 5.36 ($SD = 1.66 \sigma$). Based on this statistical feature, a year with >7 MTC events (which corresponds to a lower limit of the mean plus 0.8σ) was defined as an active MTC year. A year with ≤ 4 MTC events (which corresponds to an upper limit of the mean minus 0.8σ), was defined as an inactive MTC year. Years with 5 or 6 MTC events were defined as normal MTC years. Table 1 lists all active and inactive MTC years. Seven active MTC years and seven inactive MTC years were identified for the period 1979–2006.

Figure 4 illustrates each TC genesis location during all of the active and inactive MTC years. Notably, during active MTC years, the genesis region expanded farther to the north, south, and east. As a result, cyclogenesis frequencies north of $20^\circ N$, south of $10^\circ N$ and east of $160^\circ E$ were much greater in active MTC years than in inactive MTC years.

Although the correlation coefficient between the number of the MTC event and the total summer TC frequency is high, some differences between the two are evident. For example, the total TC frequency was low (only 18) in 1979, but 1979 was an active MTC year, with seven MTC events. In 1996, the total TC frequency ($n=30$) was high, but it was not an active MTC year. This indicates that high or low total summer TC frequency does not necessarily match all of the MTC events in active or inactive years.

The average numbers of the MTC events each month from June to October between the active and inactive MTC years are shown in Fig. 5. The average frequency of MTC events each month was greater in active MTC years. The maximum difference occurred in June and September, and it exceeds the 95% confidence level. Interestingly, no MTC events each occurred in earlier summer (i.e., June) during inactive years, whereas there was no obvious difference between active and inactive years in October. In the following analysis, we reveal the composite difference of large-scale dynamic and thermodynamic fields between active and inactive MTC years.

Table 1. List of the number of the MTC events, the number of TCs associated with the MTC events and total TC frequency during June–October for seven active and inactive MTC years.

	Year	MTC events	TC associated with MTC	Total TC frequency
Active MTC year (7)	1992	9	19	28
	1993	8	16	25
	1979	7	16	18
	1989	7	16	26
	1990	7	15	23
	1994	7	22	33
	2004	7	15	22
Inactive MTC year (7)	1980	4	9	20
	2005	4	8	18
	1981	3	8	21
	1986	3	8	17
	1998	3	14	20
	2003	3	8	18
	1983	2	5	17

4. Circulation patterns associated with active and inactive MTC years

4.1 Seasonal mean patterns

The composite SST difference maps from the preceding winter (December–February) to the concurrent summer (June–October) between active and inactive MTC years are shown in Fig. 6. In the preceding winter, significant cold SST anomalies appeared in the equatorial central and eastern Pacific. As the TC season progresses, cold SST anomalies in the equatorial central and eastern Pacific dissipate. By the concurrent summer, the SST anomalies in the equatorial central Pacific became positive, while the cold SST anomalies occurred in the western Pacific. Such an evolution resembles a typical ENSO decaying phase.

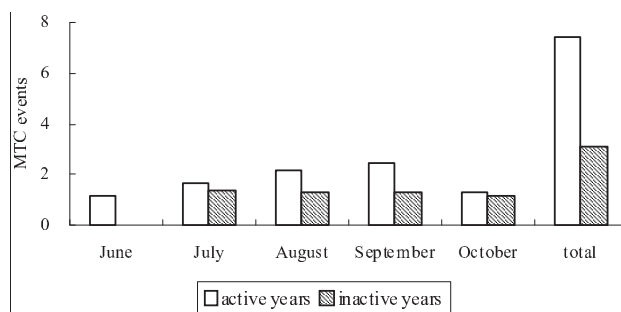


Fig. 5. Average number of the MTC events from June to October between the MTC active (white bar) and inactive (gray bar) years. In case a MTC event passes two months, counted to the month in which the MTC event had a longer period.

This result suggests that ENSO may have a delayed impact on the summer MTC activity in the WNP, possibly through a local thermodynamic atmosphere–ocean feedback, as discussed by Wang et al. (2003) and Wu et al. (2009, 2010a, b).

To what extent does the ENSO control the interannual variation of the MTC frequency? To address this question, we examined 3-month running-mean SST anomalies in the Niño-3.4 region (5°N–5°S, 120°–170°W) in active MTC and inactive years (Table 2). The relationship with ENSO is quite complicated.

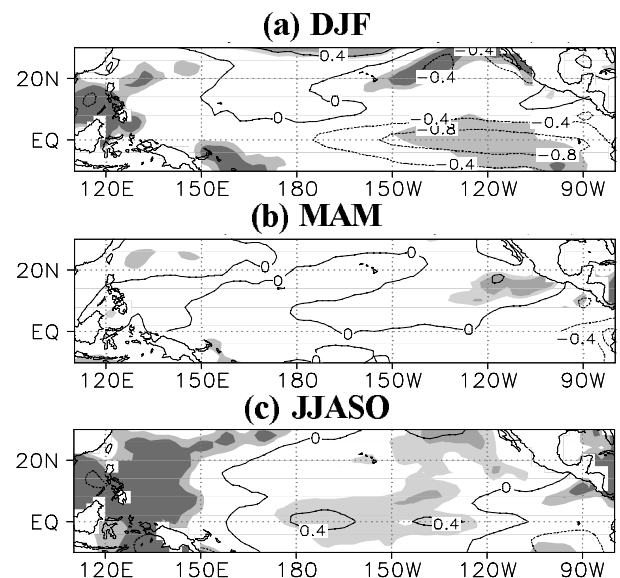


Fig. 6. Composite SST difference patterns between active and inactive MTC years from the preceding DJF to the concurrent JJASO. Shading indicates the area exceeding 95% (darker color) and 90% (lighter color) confidence levels.

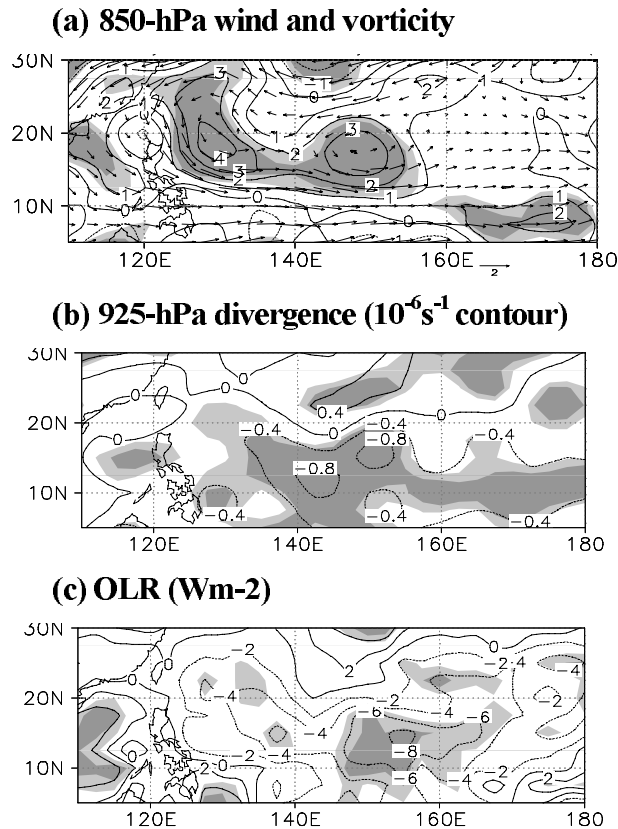


Fig. 7. Composite differences of (a) 850-hPa wind (vector, m s⁻¹) and vorticity (contour, 10⁻⁶ s⁻¹) fields, (b) 925-hPa divergence (contour, 10⁻⁶ s⁻¹), and (c) OLR (W m⁻²) between active and inactive MTC years during June–October. Shading indicates the area exceeding 95% (darker color) and 90% (lighter color) confidence levels.

In inactive MTC years, four of seven years are related to the El Niño decaying phase, two years (1980, 1981) are neutral or non-ENSO (when the amplitude of the average Niño-3.4, anomaly of SST is <0.5°C) years, and one year (1986) is associated with the El Niño developing phase. In active MTC years, four of seven years were related to ENSO (either in the El Niño developing/maintaining phase or the La Niña decaying phase), whereas three other years (1990, 1993, 1979) are neutral years. This data suggests that although the year-to-year change of frequency of MTC events is somehow correlated with ENSO variation, ENSO is not a sole factor affecting MTC frequency. Local or other remote forcing processes must come into play.

Next, we examined the composite atmospheric circulation difference between active and inactive MTC years. Figure 7 illustrates the composite differences of 850-hPa wind and vorticity, 925-hPa divergence, and OLR fields between active and inactive MTC years. Because the patterns of the composite wind and vorticity anomalies are approximately a mirror image be-

tween active and inactive years, only the difference field is shown. Notably, a low-level cyclonic circulation anomaly appears over the South China Sea (SCS) and the WNP during the active MTC years and an anticyclonic circulation anomaly appears over these regions during inactive years (Fig. 7a). The first baroclinic mode of anomalous circulation has an approximately vertical structure, with an anticyclonic or cyclonic circulation anomaly appearing in the upper troposphere (at 200 hPa), even though the difference in the upper tropospheric wind is not statistically significant. The low-level cyclonic vorticity developed in the preceding winter and persisted from the winter to the following summer (figure not shown); this pattern is a mirror image of the typical WNP circulation change during the ENSO decaying phase (Wang et al., 2003; Wu et al., 2009, 2010a, b). As discussed in Wang et al. (2003), an anomalous anticyclone in the WNP can persist from a mature El Niño winter to the subsequent spring and summer, whereas a cyclone can persist from a mature La Niña winter. On one hand, a local, positive thermodynamic atmosphere–ocean feedback can maintain the anomalous anticyclone or cyclone from boreal winter to spring (Wang et al., 2003). As the WNP monsoon starts, the local cold SST anomaly may suppress the monsoon convection, leading to a weak monsoon; the local warm SST anomaly may enhance convection, leading to a strong monsoon (Wu et al., 2010a). On the other hand, the Indian Ocean basin-wide warming resulting from El Niño forcing may further strengthen the WNP anticyclone anomaly, or cooling from La Niña forcing may further strengthen the cyclone (Xie et al., 2009). As a consequence of the positive low-level cyclonic vorticity anomaly (Fig. 7a), the WNP monsoon trough strengthened and extended eastward during active MTC years, which favored MTC genesis farther east.

The difference with the low-level vorticity field is consistent with the 925-hPa divergence and the OLR difference fields (Figs. 7b and c). Significant differences in the large-scale, low-level convergence and convection are found in the WNP between active and inactive MTC years. Figure 7c illustrates that convection greatly strengthens along the WNP monsoon trough during active MTC years. Such strengthening provides a favorable thermodynamic condition for MTC genesis.

4.2 ISO intensity

How does the atmospheric ISO change during active MTC and inactive years? To address the question, we calculated the averaged summer ISO intensity during active and inactive years. Here the ISO intensity was measured based on the standard deviation of 25–70-day band-pass-filtered OLR field during June–

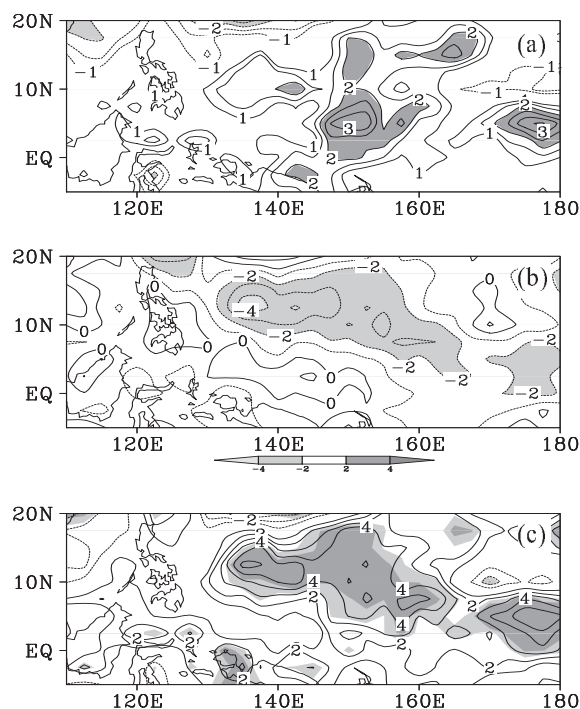


Fig. 8. ISO intensity (unit: W m^{-2}) fields composed based on active (a) and inactive (b) MTC years and their difference (c). The ISO intensity with a value $>2 \text{ W m}^{-2}$ or $<-2 \text{ W m}^{-2}$ is shaded in the top and middle panels. Shading in the bottom panel indicates the area exceeding 95% (darker color) and 90% (lighter color) confidence levels.

October. Figure 8 shows the ISO intensity fields based on active and inactive MTC years and their differences. Notably, during active MTC years, ISO was greatly enhanced over the equatorial region from 125°E to 150°E and the off-equatorial WNP region from 130°E to 165°E , from 5°N to 20°N (Fig. 8a). The composite field of inactive MTC years, on the other hand, shows a nearly opposite pattern (Fig. 8b). ISO greatly weakened in both the equatorial region and the off-equatorial WNP region. This difference is statistically significant (Fig. 8c). This result suggests that the atmospheric ISO plays an important role in regulating the MTC events. Large-scale circulation anomalies associated with the strengthened ISO convective activity may favor the genesis of MTC events.

Because the summer ISO undergoes pronounced eastward propagation along the equator and northward and northwestward propagation in the off-equatorial region, we further investigated the differences in propagation characteristics of ISO between active and inactive MTC years. Because the BSISO has a large-scale spatial pattern, its maximum energy spectrum is confined in the lowest wavenumbers (Lin and Li, 2008). Thus, in the following ISO spectrum

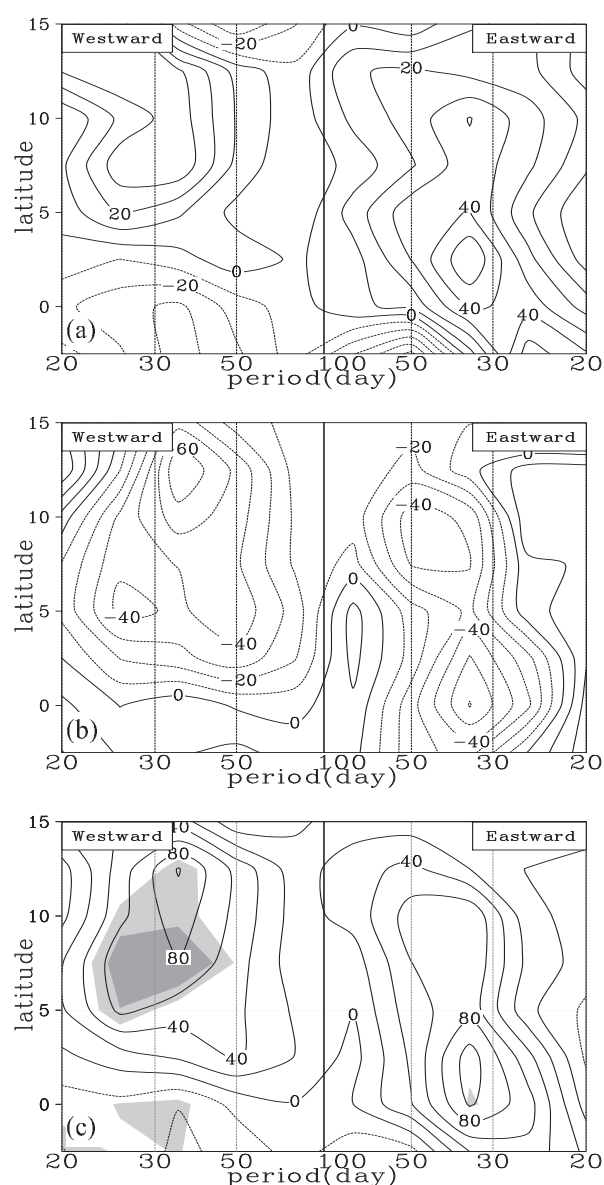


Fig. 9. Anomalous energy spectrum of the zonal wavenumber-1 and -2 eastward- and westward-propagating BSISOs during active (a) and inactive (b) MTC years and their difference (c). Shading in the bottom panel indicates 95% (darker color) and 90% (lighter color) confidence levels.

discussion we focus on the zonal or meridional wavenumber-1 and -2 modes.

Figure 9 shows the anomalous energy spectrum of the wavenumber-1 and -2 eastward- and westward-propagating BSISO modes during active and inactive MTC years and their differences. Here, the anomalous spectrum was defined as the difference from the 28-year composite. Notably, the eastward-propagating ISO mode strengthened in both the equatorial and

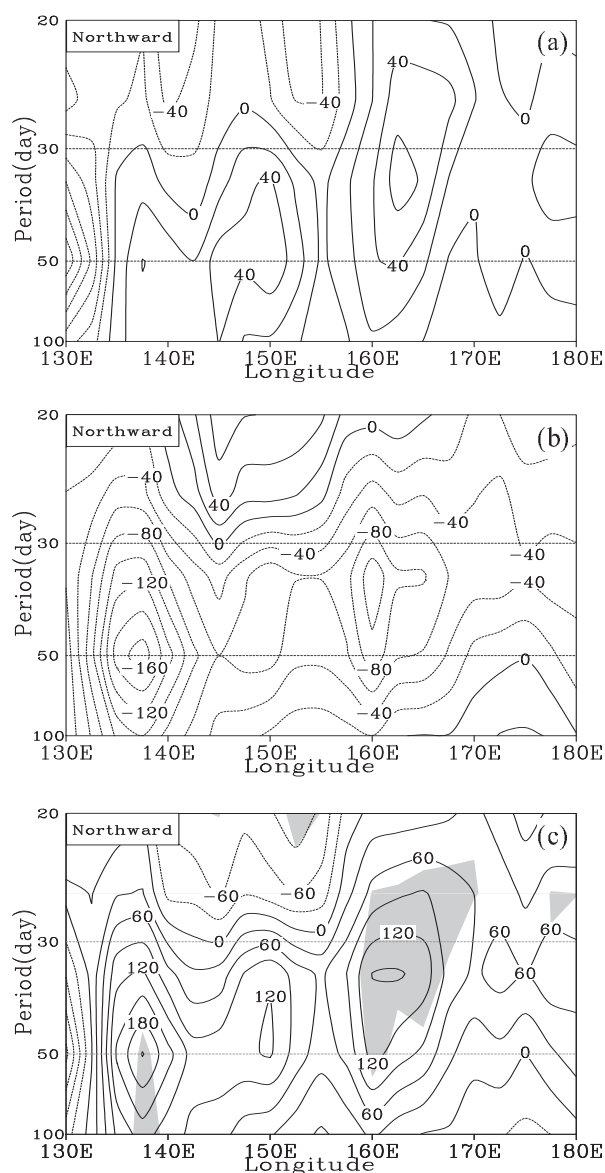


Fig. 10. Anomalous energy spectrum of the wavenumber-1 and -2 northward-propagating BSISOs during active (a) and inactive (b) MTC years and their difference (c). Shading in the bottom panel indicates a 90% confidence level.

the off-equatorial regions during active MTC years (Fig. 9a), whereas it weakened in inactive MTC years (Fig. 9b). The maximum energy spectrum difference existed in the equatorial region (-5°S – 5°N). Meanwhile, the westward-propagating ISO mode strengthened in the off-equatorial region during active MTC years (Fig. 9a) but weakened in inactive MTC years (Fig. 9b). The difference map (Fig. 9c) shows a significant change in the off-equatorial region (5° – 15°N) during the intraseasonal (25–70-day) period.

Compared to the anomalous spectrum of the zonal

propagating mode, greater variability appeared in the meridional propagating mode (Fig. 10). During active MTC years, the northward propagation was greatly enhanced over 130° – 180°E at a dominant period of 25–70 days, whereas northward propagation was suppressed during inactive years. The most significant difference between the active and inactive years appeared in the WNP region around 150° – 170°E at the 25–70-day band (Fig. 10c).

To examine the overall interannual relationship between the number of MTC events and the ISO spectrum, we defined a northward-propagation and a westward-propagation ISO intensity index. The northward-propagation index is defined as an average value of the northward-propagating 25–70-day spectrum at 150° – 170°E , and the westward-propagation index is defined as an averaged spectrum of the wavenumber-1 and -2 at 5° – 15°N for the same period of 25–70 days. Figure 11 shows a scatter diagram between the number of the MTC events and the northward/westward propagation intensity index for the entire 28-year period. The overall trend reveals an in-phase relationship between the ISO propagation strength and the yearly number of the MTC events; that is, the ISO northward-propagation in the western Pacific and the westward-propagation in the off-equatorial region was enhanced with the increased MTC events. Physically, it has been argued that the strengthening of the seasonal-mean large-scale convection and the monsoon trough in the WNP leads to enhanced westward and northward propagating ISO activity (Lin and Li, 2008), and that both the mean

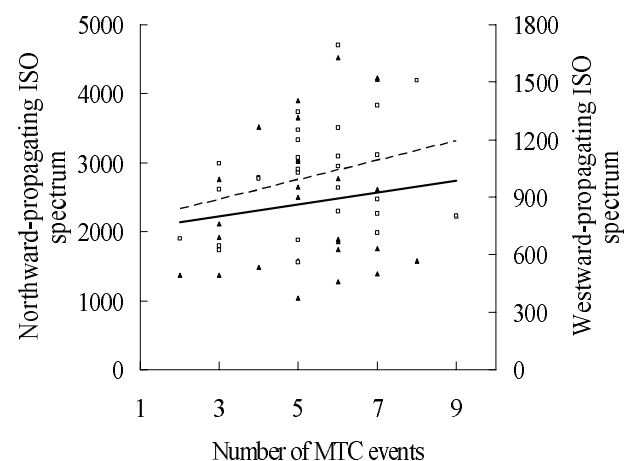


Fig. 11. Scatter diagram between the number of MTC events and the northward-propagating ISO intensity index (triangles, with the solid line denoting its linear trend) and the westward-propagating ISO intensity index (squares, with the dashed line denoting its linear trend) each year during 1979–2006.

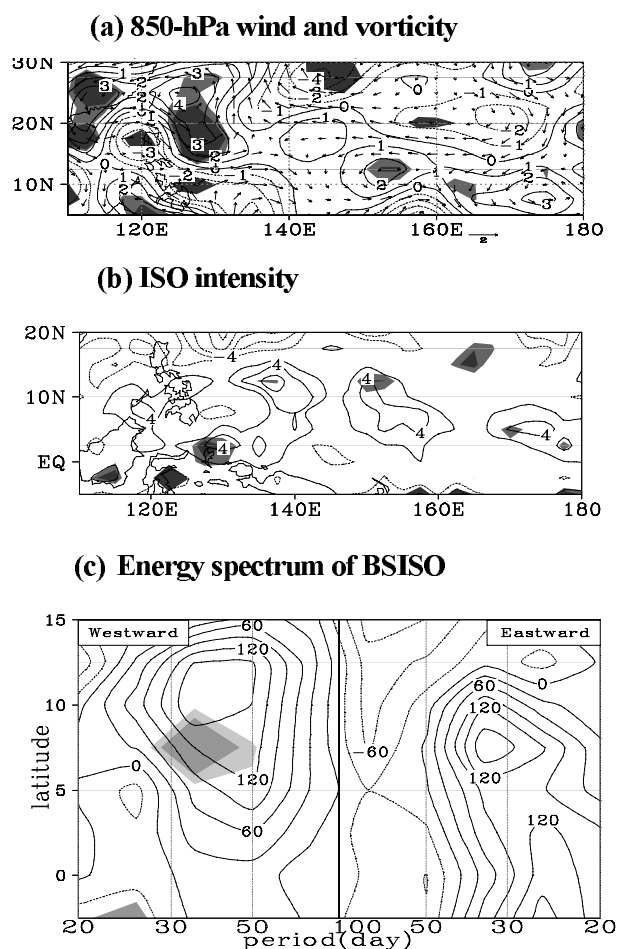


Fig. 12. Composite differences of (a) 850-hPa wind (vector, m s^{-1}) and vorticity (contour, 10^{-6} s^{-1}) fields, (b) ISO intensity (unit: W m^{-2}), and (c) energy spectrum of the zonal wavenumber-1 and -2 eastward- and westward-propagating BSISOs between active and inactive MTC years during June–October when only neutral years are considered. Shading indicates the area exceeding the 95% (darker color) and 90% (lighter color) confidence levels.

flow and ISO changes promote favorable dynamic and thermodynamic background conditions for the generation of MTC events.

5. Discussion

Our calculations show that a simultaneous correlation between the summer MTC frequency and the Niño-3.4 SSTA index for the period 1979–2006 is not statistically significant. Both active and inactive MTC years can occur even when the eastern equatorial Pacific SSTA is in a normal state (Table 2). In fact, three neutral years (1993, 1979, and 1990) were identified as active MTC years, and two neutral years (1980 and 1981) were identified as inactive MTC years. These

results suggest that ENSO is not the sole factor that controls the yearly occurrence of the MTC events.

To identify significant large-scale circulation differences in these non-ENSO cases between active and inactive MTC years, we conducted an additional composite analysis. The composite differences of 850-hPa wind and vorticity fields as well as the ISO intensity during June–October between active and inactive MTC years (with only five neutral years) were considered (Fig. 12). Notably, during the active MTC years, positive low-level cyclonic vorticity anomaly and enhanced ISO intensity appeared over the WNP region. The spectrum analysis shows that the BSISO westward propagation in the off-equatorial WNP region strengthened. The difference fields are statistically significant in some of the WNP regions. The result implies that even in the absence of ENSO, the favorable large-scale circulation and strengthened ISO activity may still occur. The source of the large-scale circulation change in this case may have arisen from local or other remote forcing factors.

The composite SSTA evolution (Fig. 6) primarily reflects the four inactive MTC years (1998, 1983, 2003, and 2005), all of which were concurrent with an El Niño decaying phase. By separating ENSO phases, Lin and Li (2008) showed that the BSISO intensity differs significantly in the ENSO developing and decaying phases. An enhanced northward- and eastward-propagating ISO spectrum appeared during an El Niño developing summer, whereas a weakened ISO spectrum appeared during an El Niño decaying summer, consistent with our results. The seasonal mean circulation anomalies showed similar ENSO-phase dependence: suppressed convection and low-level anti-cyclonic (cyclonic) flow occurred during the El Niño decaying phase, and enhanced convection and low-level cyclonic flow occurred during the El Niño developing phase (Wang et al., 2003; Li, 2010). Therefore, the temporal evolution of eastern Pacific SSTAs from the preceding winter to the concurrent summer rather than the simultaneous SSTA determines the seasonal mean circulation anomaly and the ISO intensity change in the WNP.

How does the ISO dynamically influence the MTC events? An observational analysis by Hsu et al. (2011) showed that the ISO flow may affect the synoptic-scale activity (including TC activity) through barotropic energy conversion. They noted that both the ISO low-level rotational and divergent flows enhanced barotropic energy conversion from the background flow to synoptic eddies during an ISO active phase. Given the marked intraseasonal (20–90-day) periodicity, ISO may exert a low-frequency modulation of synoptic wave and TC activity. The circulation and

Table 2. Three-month-running-mean ERSST.v3b SST anomalies in the Niño-3.4 region (5°N – 5°S , 120° – 170°W) during seven active and inactive MTC years. Bold numbers highlight El Niño and La Niña episodes defined when the SST anomalies exceed the threshold of $\pm 0.5^{\circ}\text{C}$ for a minimum of five consecutive overlapping seasons.

	Year	DJF	JFM	FMA	MAM	AMJ	MJJ	JJA	JAS	ASO	SON	OND	NDJ
Active Years	1992	1.8	1.6	1.5	1.4	1.2	0.8	0.5	0.2	0	−0.1	0	0.2
	1993	0.3	0.4	0.6	0.7	0.8	0.7	0.4	0.4	0.4	0.4	0.3	0.2
	1979	−0.1	0	0.1	0.1	0.1	−0.1	0	0.1	0.3	0.4	0.5	0.5
	1989	−1.7	−1.5	−1.1	−0.8	−0.6	−0.4	−0.3	−0.3	−0.3	−0.3	−0.2	−0.1
	1990	0.1	0.2	0.2	0.2	0.2	0.2	0.3	0.3	0.3	0.3	0.3	0.4
	1994	0.2	0.2	0.3	0.4	0.5	0.5	0.6	0.6	0.7	0.9	1.2	1.3
	2004	0.4	0.3	0.2	0.2	0.3	0.5	0.7	0.8	0.9	0.8	0.8	0.8
Inactive years	1980	0.5	0.3	0.2	0.2	0.3	0.3	0.2	0	−0.1	−0.1	0	−0.1
	2005	0.7	0.5	0.4	0.4	0.4	0.4	0.4	0.3	0.2	−0.1	−0.4	−0.7
	1981	−0.3	−0.5	−0.5	−0.4	−0.3	−0.3	−0.4	−0.4	−0.3	−0.2	−0.1	−0.1
	1986	−0.5	−0.4	−0.2	−0.2	−0.1	0	0.3	0.5	0.7	0.9	1.1	1.2
	1998	2.3	1.9	1.5	1	0.5	0	−0.5	−0.8	−1	−1.1	−1.3	−1.4
	2003	1.2	0.9	0.5	0.1	−0.1	0.1	0.4	0.5	0.6	0.5	0.6	0.4
	1983	2.3	2	1.5	1.2	1	0.6	0.2	−0.2	−0.6	−0.8	−0.9	−0.7

moisture anomalies during an active ISO period may promote a favorable environment for the generation of the MTC events.

Studies by Wang and Fan (2006) and Wang et al. (2007) showed a significant simultaneous correlation between WNP TC frequency and AAO/NPO index. To determine whether or not such a relationship exists for MTC events, we calculated correlation coefficients of the summer MTC frequency using the AAO/NPO index in the preceding winter (DJF) and spring (MAM) and the concurrent summer (JJASO) for the period 1979–2006. The correlation analysis results show no significant simultaneous relationship between the MTC frequency and the AAO or the NPO. The correlation coefficients are 0.05 and -0.01 . The correlations with the AAO index in the preceding winter and spring are also statistically insignificant. The correlation coefficients are only 0.06 and 0.07. The only significant correlation (0.39) was found between the NPO index in the preceding spring. The specific process through which the NPO in the preceding spring affects the summer MTC frequency is not clear at the moment, and it deserves further observational and modeling studies.

6. Conclusion

In this study, a multiple tropical cyclone (MTC) event was defined based on the statistics of TC genesis frequency during the June–October for the period 1979–2006 in the WNP, as derived from the JTWC best-track data. This definition was based on both the time interval and the relative location of two successive TCs. The number of so-defined summer MTC events ranged from two to nine per year, exhibiting

a pronounced interannual variation. For the period 1979–2006, the average number of active MTC events per year was 5.36 ($\text{SD} = 1.66 \sigma$). Based on this statistical feature, we defined an active MTC year as one in which ≥ 7 MTC events occurred, an inactive MTC year was one in which ≤ 4 MTC events appeared, and an MTC normal year was one in which the number of the MTC events was 5 or 6. With the criterion, seven active and seven inactive MTC years were identified during the period 1979–2006. Compared with inactive MTC years, TC genesis locations during active MTC years extended farther to the east and in the meridional direction. The maximum difference of average MTC frequency between active and inactive MTC years occurred in June, August, and September.

The composite differences of large-scale SST and circulation patterns between active and inactive MTC years showed that inactive MTC years are often associated with a warm SST anomaly in the equatorial central-eastern Pacific in the preceding winter. As the season progresses from the winter to the concurrent summer, the SST transitions from a warm to a cold anomaly. This SST evolution characteristic resembles a typical El Niño decaying phase. Weakened low-level cyclonic and upper-level anticyclonic vorticity and suppressed large-scale convection along the WNP monsoon trough are associated with this SST evolution. An opposite pattern appears during active MTC years, but the number of such events is much less.

In addition to the mean flow difference, significant differences are also found in the intraseasonal variability. Compared to inactive MTC years, ISO convective activity is greatly strengthened along the equator and in the WNP region during active MTC years. A

finite-domain wavenumber-frequency analysis was performed to examine the difference of propagation features of ISO between active and inactive MTC years. The results show that both the ISO westward propagation in the off-equatorial region and the northward propagation over the WNP strengthened during active MTC years and weakened during inactive MTC years. Thus both the enhanced mean monsoon trough and the strengthened ISO activity may set up a favorable environment for the generation of MTC events.

The overall relationship between the number of MTC events and the northward- and westward-propagating ISO intensity indices during the entire 28-yr period exhibits an in-phase relationship. This correlation implies that the enhanced westward propagation in the off-equatorial region and the enhanced northward propagation in the western Pacific could result in more frequent MTC events in the WNP.

Acknowledgements. This work was conducted during a visit by GAO Jianyun to International Pacific Research Center. GAO Jianyun was supported by National Natural Science Foundation of China (Grant Nos. 90915002 and 40775047), by the Youth Project of Fujian Provincial Department of Science & Technology (Grant No. 2007F3019), by the Science and Technology Key Project of Fujian Province (Grant No. 2011Y0008), and by the open-end fund project of Fujian Provincial Meteorological Bureau (Grant No. 2010K05). LI Tim was supported by Office of Naval Research (Grant Nos. N000140810256 and N000141010774), and by the International Pacific Research Center that was sponsored by the Japan Agency for Marine-Earth Science and Technology (JAMSTEC), NASA (Grant No. NNX07AG53G) and NOAA (Grant No. NA17RJ1230). This is SOEST contribution number 8723 and IPRC contribution number 903.

REFERENCES

- Briegleb, L. M., and W. M. Frank, 1997: Large-scale influences on tropical cyclogenesis in the western North Pacific. *Mon. Wea. Rev.*, **125**, 1397–1413.
- Camargo, S. J., and A. H. Sobel, 2005: Western north Pacific tropical cyclone intensity and ENSO. *J. Climate*, **18**, 2996–3006.
- Camargo, S. J., K. A. Emanuel, and A. H. Sobel, 2007a: Use of a genesis potential index to diagnose ENSO effects on tropical cyclone genesis. *J. Climate*, **20**, 4819–4834.
- Camargo, S. J., A. H. Sobel, A. G. Barnston, and K. A. Emanuel, 2007b: Tropical cyclone genesis potential index in climate models. *Tellus*, **59A**, 428–443.
- Camargo, S. J., A. W. Robertson, S. J. Gaffney, P. Smyth, and M. Ghil, 2007c: Cluster analysis of typhoon tracks. Part II: Large-scale circulation and ENSO. *J. Climate*, **20**, 3654–3676.
- Chan, J. C. L., 1985: Tropical cyclone activity in the Northwest Pacific in relation to the El Niño/Southern Oscillation phenomenon. *Mon. Wea. Rev.*, **113**, 599–606.
- Chang, C.-P., V. F. Morris, and J. M. Wallace, 1970: A statistical study of easterly waves in the western Pacific: July–December 1964. *J. Atmos. Sci.*, **27**, 195–201.
- Chang, C.-P., J. M. Chen, P. A. Harr, and L. E. Carr, 1996: North-westward-propagating wave patterns over the tropical western North Pacific during summer. *Mon. Wea. Rev.*, **124**, 2245–2266.
- Chen, T.-C., and J.-M. Chen, 1993: The 10–20-day mode of the 1979 Indian monsoon: Its relation with the time variation of monsoon rainfall. *Mon. Wea. Rev.*, **121**, 2465–2482.
- Chen, T.-C., S.-P. Weng, N. Yamazaki, and S. Kiehne, 1998: Interannual variation in the TC formation over the western North Pacific. *Mon. Wea. Rev.*, **126**, 1080–1090.
- Chen, T.-C., M.-C. Yen, and S.-P. Weng, 2000: Interaction between the summer monsoons in East Asia and the South China Sea: Intraseasonal monsoon modes. *J. Atmos. Sci.*, **57**, 1373–1392.
- Chia, H. H., and C. F. Ropelewski, 2002: The interannual variability in the genesis location of tropical cyclones in the Northwest Pacific. *J. Climate*, **15**, 2934–2944.
- Dickinson, M., and J. Molinari, 2002: Mixed Rossby-gravity waves and western Pacific tropical cyclogenesis. Part I: Synoptic evolution. *J. Atmos. Sci.*, **59**, 2183–2195.
- Duchon, C. E., 1979: Lanczos filter in one and two dimensions. *J. Appl. Meteor.*, **18**, 1016–1022.
- Fan, K., 2007: North Pacific sea ice cover, a predictor for the western North Pacific typhoon frequency? *Science in China (D)*, **50**(8), 1251–1257.
- Frank, W. M., and P. E. Roundy, 2006: The role of tropical waves in tropical cyclogenesis. *Mon. Wea. Rev.*, **134**, 2397–2417.
- Fu, B., T. Li, M. S. Peng, and F. Weng, 2007: Analysis of tropical cyclogenesis in the western north pacific for 2000 and 2001. *Wea. Forecasting*, **22**, 763–780.
- Gao, J.-Y., and T. Li, 2010: Factors controlling multiple tropical cyclone events in western North Pacific. *Mon. Wea. Rev.*, **139**, 885–894.
- Gray, W. M., 1968: Global view of the origin of tropical disturbances and storms. *Mon. Wea. Rev.*, **96**, 669–700.
- Gray, W. M., 1977: Tropical cyclone genesis in the western North Pacific. *J. Meteor. Soc. Japan*, **55**, 465–482.
- Harr, P. A., and R. L. Elsberry, 1995a: Large-scale circulation variability over the tropical western North Pacific Part I: Spatial patterns and tropical cyclone characteristics. *Mon. Wea. Rev.*, **123**, 1225–1246.
- Harr, P. A., and R. L. Elsberry, 1995b: Large-scale circulation variability over the tropical western North Pacific. Part II: Persistence and transition characteristics. *Mon. Wea. Rev.*, **123**, 1247–1268.

- Hayashi, Y., 1982: Space-time spectral analysis and its applications to atmospheric waves. *J. Meteor. Soc. Japan*, **60**, 156–171.
- Hendon, H. H., M. C. Wheeler, and C. Zhang, 2007: Seasonal dependence of the MJO–ENSO relationship. *J. Climate*, **20**, 531–543.
- Hsu, P.-C., T. Li, and C.-H. Tsou, 2011: Interactions between boreal summer intraseasonal oscillations and synoptic-scale disturbances over the western North Pacific. Part I: Energetics diagnosis. *J. Climate*, **24**, 927–941.
- Hsu, P.-C., and T. Li, 2011: Interactions between boreal summer intraseasonal oscillations and synoptic-scale disturbances over the western North Pacific. Part II: Apparent heat and moisture sources and Eddy momentum transport. *J. Climate*, **24**, 942–961.
- Holland, G. J., 1995: Scale interaction in the western Pacific monsoon. *Meteor. Atmos. Phys.*, **56**, 57–79.
- Kalnay, E., and Coauthors, 1996: The NCEP/NCAR 40-Year Reanalysis Project. *Bull. Amer. Meteor. Soc.*, **77**, 437–471.
- Kanamitsu, M., W. Ebisuzaki, J. Woollen, S.-K. Yang, J. J. Hnilo, M. Fiorino, and G. L. Potter, 2002: NCEP–DOE AMIP-II Reanalysis (R-2). *Bull. Amer. Meteor. Soc.*, **83**, 1631–1643.
- Kim, J.-H., C.-H. Ho, H.-S. Kim, C.-H. Sui, and S. K. Park, 2008: Systematic variation of summertime tropical cyclone activity in the western North Pacific in relation to the Madden–Julian Oscillation. *J. Climate*, **21**, 1171–1191.
- Kiladis, G. N., and M. Wheeler, 1995: Horizontal and vertical structure of observed tropospheric equatorial Rossby waves. *J. Geophys. Res.*, **100**, 22981–22997.
- Krishnamurti, T. N., and H. N. Bhalme, 1976: Oscillations of a monsoon system. Part I: Observational aspects. *J. Atmos. Sci.*, **33**, 1937–1954.
- Krishnamurti, T. N., and P. Ardanuy, 1980: 10- to 20-day westward propagating mode and “Breaks in the Monsoons”. *Tellus*, **32**, 15–26.
- Krouse, K. P., and A. H. Sobel, 2010: An observational study of multiple tropical cyclone events in the western north Pacific. *Tellus*, **62A**, 256–265.
- Kuo, H.-C., J.-H. Chen, R. T. Williams, and C.-P. Chang, 2001: Rossby waves in zonally opposing mean flow: Behavior in Northwest Pacific summer monsoon. *J. Atmos. Sci.*, **58**, 1035–1050.
- Lander, M. A., 1994: An exploratory analysis of the relationship between tropical storm formation in the western North Pacific and ENSO. *Mon. Wea. Rev.*, **122**, 636–651.
- Lau, K.-H., and N.-C. Lau, 1990: Observed structure and propagation characteristics of tropical summertime synoptic scale disturbances. *Mon. Wea. Rev.*, **118**, 1888–1913.
- Lau, K.-M., and S. Shen, 1988: On the dynamics of intraseasonal oscillations and ENSO. *J. Atmos. Sci.*, **45**, 1781–1797.
- Li, T., 2006: Origin of the summertime synoptic-scale wave train in the western North Pacific. *J. Atmos. Sci.*, **63**(3), 1093–1102.
- Li, T., 2010: Monsoon climate variabilities. *Climate Dynamics: Why Does Climate Vary? Geophys. Monogr. Ser.*, D.-Z. Sun and B. Frank, Eds., doi: 10.1029/2008GM000782.
- Li, T., and B. Wang, 1994: The influence of sea surface temperature on the tropical intraseasonal oscillation: A numerical experiment. *Mon. Wea. Rev.*, **122**, 2349–2362.
- Li, T., and B. Fu, 2006: Tropical cyclogenesis associated with Rossby wave energy dispersion of a preexisting typhoon. Part I: Satellite data analyses. *J. Atmos. Sci.*, **63**, 1377–1389.
- Li, T., B. Fu, X. Ge, B. Wang, and M. Ping, 2003: Satellite data analysis and numerical simulation of tropical cyclone formation. *Geophys. Res. Lett.*, **30**, 2122–2126.
- Liebmann, B., and C. A. Smith, 1996: Description of a complete (interpolated) outgoing longwave radiation dataset. *Bull. Amer. Meteor. Soc.*, **77**, 1275–1277.
- Liebmann, B., H. H. Hendon, and J. D. Glick, 1994: The relationship between tropical cyclones of the western Pacific and Indian Oceans and the Madden–Julian oscillation. *J. Meteor. Soc. Japan*, **72**, 401–412.
- Lin, A., and T. Li, 2008: Energy spectrum characteristics of boreal summer intraseasonal oscillations: Climatology and variations during the ENSO developing and decaying phases. *J. Climate*, **21**, 6304–6320.
- Maloney, E. D., and M. J. Dickinson, 2003: The intraseasonal oscillation and the energetics of summertime tropical western North Pacific synoptic-scale disturbances. *J. Atmos. Sci.*, **60**, 2153–2168.
- Murakami, M., 1976: Cloudiness fluctuations during summer monsoon. *J. Meteor. Soc. Japan*, **54**, 175–181.
- Murakami, M., and M. Frydrych, 1974: On the preferred period of upper wind fluctuations during the summer monsoon. *J. Atmos. Sci.*, **31**, 1549–1555.
- Nakazawa, T., 1986: Intraseasonal variations of OLR in the tropics during the FGGE year. *J. Meteor. Soc. Japan*, **64**, 17–34.
- Nakazawa, T., 1988: Tropical super clusters within intraseasonal variations over the western Pacific. *J. Meteor. Soc. Japan*, **66**, 823–839.
- Numaguti, A., 1995: Characteristics of 4–20-day-period disturbances observed in the equatorial Pacific during the TOGA COARE IOP. *J. Meteor. Soc. Japan*, **73**, 353–377.
- Ritchie, E. A., and G. J. Holland, 1999: Large-scale patterns associated with tropical cyclogenesis in the western Pacific. *Mon. Wea. Rev.*, **127**, 2027–2043.
- Saunders, M. A., R. E. Chandler, C. J. Merchant, and F. P. Roberts, 2000: Atlantic hurricanes and NW Pacific typhoons: ENSO spatial impacts on occurrence and landfall. *Geophys. Res. Lett.*, **27**(8), 1147–1150.
- Shi, L., A. Oscar, H. H. Hendon, G. Wang, and D. Anderson, 2009: The role of stochastic forcing in ensemble forecasts of the 1997/98 El Niño. *J. Climate*, **22**, 2526–2540.
- Sobel, A. H., and C. S. Bretherton, 1999: Development

- of synoptic-scale disturbances over the summertime tropical northwest Pacific. *J. Atmos. Sci.*, **56**, 3106–3127.
- Sobel, A. H., and E. D. Maloney, 2000: Effect of ENSO and the MJO on western north Pacific tropical cyclones. *Geophys. Res. Lett.*, **27**, 1739–1742.
- Takayabu, Y. N., and T. Nitta, 1993: 3–5 day period disturbances coupled with convection over the tropical Pacific Ocean. *J. Meteor. Soc. Japan*, **71**, 221–246.
- Tam, C.-Y., and T. Li, 2006: The origin and dispersion characteristics of the observed tropical summertime synoptic-scale waves over the western Pacific. *Mon. Wea. Rev.*, **134**, 1630–1646.
- Teng, H., and B. Wang, 2003: Interannual variations of the boreal summer intraseasonal oscillation in the Asian-Pacific region. *J. Climate*, **16**, 3571–3584.
- Waliser, D., 2006: Intraseasonal variations. *The Asian Monsoon*, B. Wang, Ed., Springer, 787pp.
- Wang, B., and J. C. L. Chan, 2002: How strong ENSO events affect tropical storm activity over the western North Pacific. *J. Climate*, **15**, 1643–1658.
- Wang, B., and X. Xie, 1997: A model for the boreal summer intraseasonal oscillation. *J. Atmos. Sci.*, **54**, 72–86.
- Wang, B., R. Wu, and T. Li, 2003: Atmosphere–warm ocean interaction and its impact on Asian–Australian monsoon variation. *J. Climate*, **16**, 1195–1211.
- Wang, H. J., J. Sun, and K. Fan, 2007: Research on the relationship between the North Pacific oscillation and the frequency of tropical cyclone/hurricane. *Science in China (D)*, **37**, 966–973.
- Wang, H. J., and K. Fan, 2006: The relationship between the frequency of the tropical cyclone in the western North Pacific and Antarctic oscillation. *Chinese Science Bulletin*, **51**, 2910–2914.
- Wang, H. J., and K. Fan, 2007a: Relationship between the Antarctic oscillation and the western North Pacific typhoon frequency. *Chinese Science Bulletin*, **52**(4), 561–565.
- Wang, H. J., and K. Fan, 2007b: Relationships between the North Pacific Oscillation and typhoon and hurricane frequencies. *Science in China (D)*, **50**(9), 1409–1416.
- Wu, B., T. Zhou, and T. Li, 2009: Contrast of rainfall–SST relationships in the western North Pacific between the ENSO-developing and ENSO-decaying summers. *J. Climate*, **22**, 4398–4405.
- Wu, B., T. Li, and T. Zhou, 2010a: Relative contributions of the Indian Ocean and local SST anomalies to the maintenance of the western North Pacific anomalous anticyclone during El Niño decaying summer. *J. Climate*, **23**, 2974–2986.
- Wu, B., T. Li, and T. Zhou, 2010b: Asymmetry of atmospheric circulation anomalies over the western North Pacific between El Niño and La Niña. *J. Climate*, **23**, 4807–4822.
- Wu, M. C., W. L. Chang, and W. M. Leung, 2004: Impacts of El Niño–Southern Oscillation events on tropical cyclone landfalling activity in the western North Pacific. *J. Climate*, **17**, 1419–1428.
- Xie, S.-P., K. Hu, J. Hafner, H. Tokinaga, Y. Du, G. Huang, and T. Sampe, 2009: Indian Ocean capacitor effect on Indo–Western Pacific climate during the summer following El Niño. *J. Climate*, **22**, 730–747.
- Zangvil, A., 1975: Upper tropospheric waves in the tropics and their association with clouds in the wavenumber–frequency domain. Ph. D. dissertation, University of California, Los Angeles, 131pp.
- Zhang, C., 2005: Madden-Julian oscillation. *Rev. Geophys.*, **43**(RG2003), doi: 10.1029/2004RG000158.
- Zhou, B., and X. Cui, 2011: Sea surface temperature east of Australia: A predictor of tropical cyclone frequency over the western North Pacific? *Chinese Science Bulletin*, **56**, 196–201.
- Zhou, B., and X. Cui, 2008: Hadley circulation signal in the tropical cyclone frequency over the western North Pacific. *J. Geophys. Res.*, **113**(D16107), doi: 10.1029/2007JD009156.
- Zhou, B., and X. Cui, and P. Zhao, 2008: Relationship between the Asian-Pacific oscillation and the tropical cyclone frequency in the western North Pacific. *Science in China (D)*, **51**(3), 380–385.